

K-mirror prototype for MICADO-SCAO module of the E-ELT

S. Thijs^a, O. Dupuis^a, E. Gendron^{a*}, F. Vidal^a, V. Deo^a, M. Cohen^b, A. Sevin^a, V. Lapereyre^a, Z. Hubert^a et T. Buey^a

^aLESIA, Observatoire de Paris, Université PSL, CNRS, Sorbonne Université, Université de Paris, 5 place Jules Janssen, 92195 Meudon, France; ^bGEPI, Observatoire de Paris, Université PSL, CNRS, 5 place Jules Janssen, 92195 Meudon, France

ABSTRACT

MICADO is one of the first light instruments for the E-ELT. It comes with a Single Conjugate AO system jointly developed by MICADO and MAORY. The SCAO system is attached to the MICADO cryostat that rotates to stabilize the field on the scientific focal plane. As a consequence, an optical de-rotator (a K-mirror) is needed in the SCAO WFS path to de-rotate the pupil in order to keep it stable on the WFS detector.

The specifications of the K-mirror were shown to be challenging during the preliminary design phase. The K-mirror requires an opto-mechanical rotation axis stable to a micrometric precision in translation ($<5\mu\text{m}$), with less than $50\mu\text{rad}$ variation in direction.

Keywords: K-mirror, E-ELT, MICADO, SCAO, WFS

1. INTRODUCTION

The design chosen to stabilize the pupil image during an observation is a classical opto-mechanical concept called “optical de-rotator” or K-Mirror, where three flat mirrors are rotating together at a given speed. The requirement on pupil stability during one observation leads to the necessity of an extremely good alignment of the pupil de-rotation sub-system, which results in a few microns of optical and mechanical axis precision. The control of the trajectory and its speed has to be tight and its parameters may be changed on the fly.

The prototyping of the K-Mirror consisted of two sub-developments: its opto-mechanics on one hand, and its controlling (software and electronics) on the other.

For the opto-mechanical development a test bench in order to align the K-mirror, together with an alignment procedure, has been set up. The opto-mechanical design of the internal part of the K-Mirror (the most critical) started with 3D printed elements so to validate the concept of its optical setup and the test-bed. In this paper we present the results obtained with a model manufactured with classical mechanical machining with a combination of aluminum parts and titanium, for the most critical parts.

For the development of the controlling a motor and an encoder with the proper accuracy had to be chosen. A study of the library used to control the motor and read the encoder via a PLC¹-Beckhoff based on the ESO standards, was done.

The main outputs of this prototyping activity were to have a K-Mirror that could be integrated in the WFS optical path and a test-bed usable for K-Mirror set-up, tools and procedures.

In this paper we describe the design of our K-mirror and we present its performance. In section 2 the optical and mechanical design is exposed. Section 3 ‘Methodology’ presents the test bench and the control system. In section 4 the final results and performance of our K-mirror are presented.

¹ PLC = Programmable Logic Controller

2. DESIGN

2.1 Optical design

The K-mirror is built out of an aluminum (and partially titanium) framework with at the inside three reflection surfaces: a flat mirror and a triangular prism with two reflecting surfaces at 120° (see Figure 1). The diameter of beam that passes through the K-mirror is 20 mm.

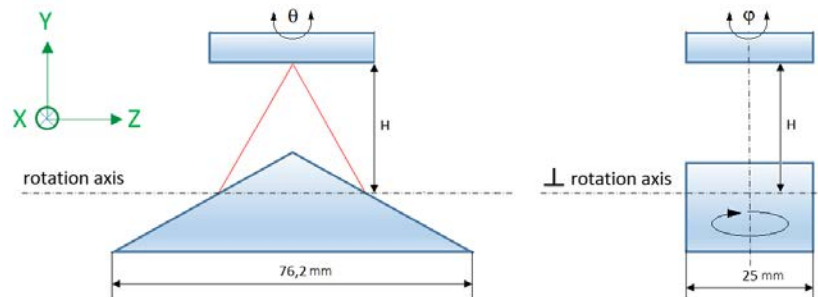


Figure 1. Flat mirror and triangular prism with two reflecting surfaces at 120° .

Although non-intuitive at first sight, it can be demonstrated that four degrees of freedom (no less, no more) are required to align the optics with respect to the mechanical rotation axis. It should be noticed also that a K-mirror can be perfectly aligned without having the plane mirror parallel to the rotation axis, or without having the faces of the prism making the same input/output angles with respect to the mechanical rotation axis; in other words, a well-aligned K-mirror does not necessarily have a “symmetrical” aspect. Moreover, four degrees of freedom are sufficient regardless of the exact value of the prism angle which is not an important nor constrained parameter. The four degrees of freedom we have chosen are:

- prism rotation ψ around Y (see Figure 1): this allows us to set the top edge of the prism orthogonal to the mechanical rotation axis,
- distance H between the mechanical rotation axis and the flat mirror,
- tip and tilt (θ and ϕ) of the plane mirror. The angle ϕ allows us to set the mirror parallel to the prism upper edge.

Other choices can be made than those presented here. Our choice is motivated by the fact that the adjustments in θ and ϕ can be done by observing an object at infinity, independently from H and ψ . On the contrary, imaging an object at a finite distance close to the K-mirror will allow us to mainly align H and ψ . Decoupling the tunings allows to reduce the number of iterations.

Having more than four degrees of freedom for the alignment necessarily leads to underdetermined problem, and consequently longer iterations and hesitations in the alignment.

2.2 Mechanical design

The K-mirror prototype is build out of three main parts:

- 1) the support structure with rotor bearings and motorization,
- 2) the internal rotor with gearwheel and scale drum and
- 3) the core structure with the optical parts.

The ‘core’ of the K-mirror that holds the prism and flat mirror (red in Figure 2), is placed in the internal rotor (yellow in Figure 2). The biggest difficulty of the mechanical design is to manage the imperfections in the linearity of the mechanical rotation axis. To reduce non-linearity, the drive shaft of the support structure and the internal rotor are mounted in abuts at the side of the motor with an elastic washer on the other side. Also the front and back face of the support structure are manufactured together to insure the alignment of the bearings.

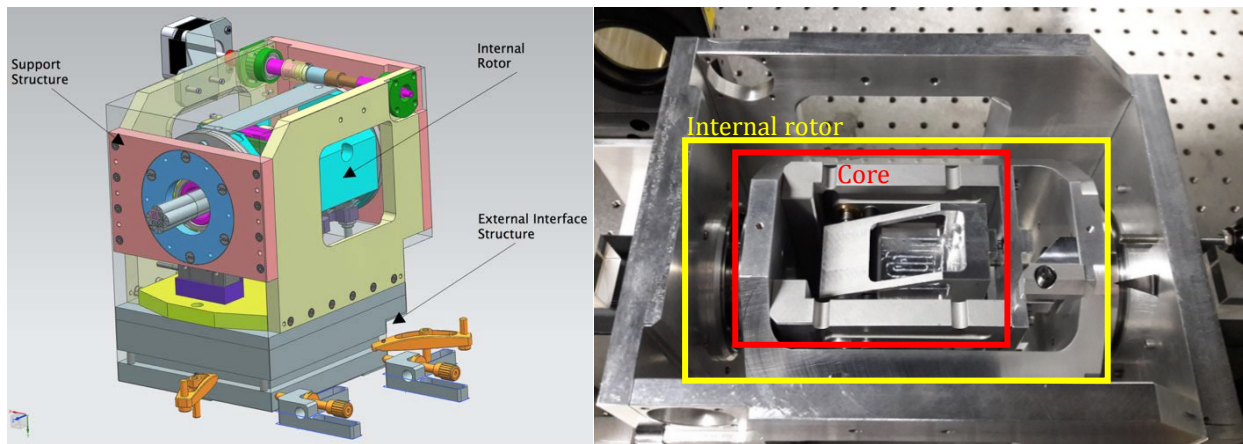


Figure 2. K-mirror with support structure, internal rotor (yellow) and core (prism and flat mirror support, red)

The other critical part is the core of the K-mirror which holds the prism and the flat mirror (see Figure 3). Both optics are independent so that the separation between them (the height) can be changed thanks to a flexor build out of titanium in order to increase its rigidity.

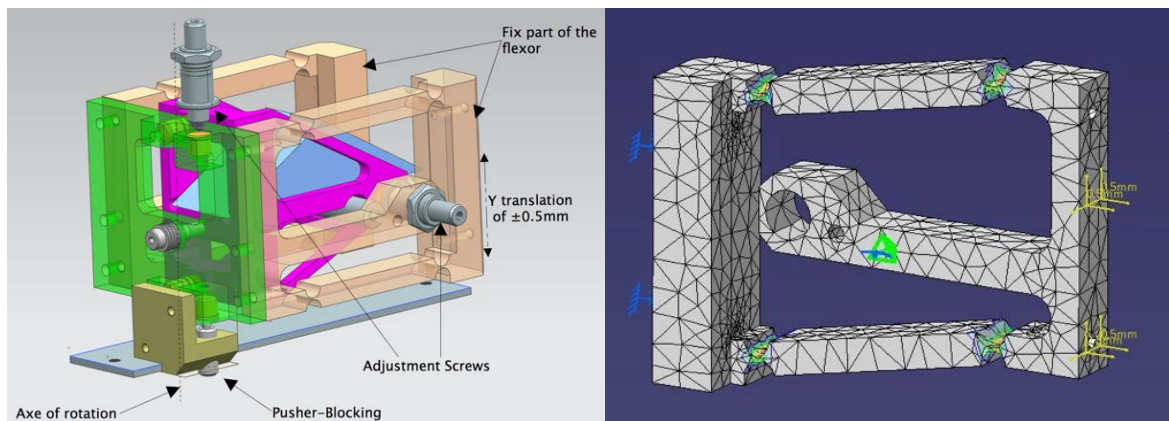


Figure 3. **Left:** Prism support and flexor. Height is changed with the vertical adjustment screw on the left in the figure. The rotation of the prism is modified with the horizontal screw on the right. **Right:** screen capture of the finite element analysis of the flexors showing the principle of motion.

The angles θ and ϕ can be adjusted using three micrometric screws with a $25 \mu\text{m}/\text{turn}$ thread pitch over $\geq 0.4\text{mm}$ travel. They can thus modify the angle with a precision better than 0.04 mrad (or $10''$). The Prism angle screw has a precision of $100\mu\text{m}/\text{turn}$ over 6mm travel or a precision of about 0.04 mrad ($10''$). The height of the prism can be changed with a precision of about $1\mu\text{m}$.

2.3 Motorization

The slow and constant rotation of the K-mirror is controlled by a stepper motor with a maximum stepping speed of 2kHz , a lost motion gearwheel and a Heidenhain scale drum with its optical head (see Figure 4). The motor has a resolution of $200 \text{ steps}/\text{turn}$ and drives the gearwheel with a factor of $1:200$, which makes a resolution of $40,000 \text{ steps per turn}$ of the rotor of the K-mirror. Assuming a micro-stepping management by the control electronics, the angular resolution is 0.16 mrad and the peak angular speed is 320 mrad/s ($18^\circ/\text{s}$).

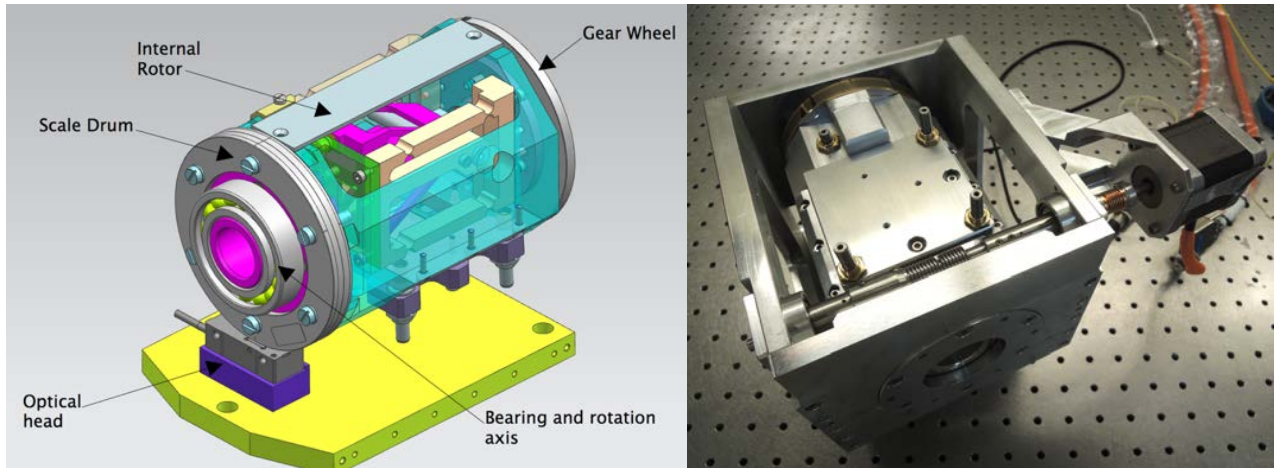


Figure 4. **Left:** internal rotor of the K-mirror with scale drum, optical head and gearwheel (lost motion gear). **Right:** final configuration.

The servo control is achieved with a Heidenhain absolute angle encoder (ECA-4000 series) with an accuracy better than 3 second of arc rms (or $14 \mu\text{rad}$ rms) at 1 second readout (4.5 times larger when operating at 20 Hz). It sends the numerical angle position via a bidirectional EnDat 2.2 interface to a specific Beckhoff terminal (EL5032) with 16 MHz clock frequency. This terminal sends a decoded value to the PLC which knows the set-point (or trajectory) and which sends the command to the ES7031 Beckhoff terminal to drive the stepper motor. The frequency of this loop is 20 Hz.

3. TEST BENCH AND METHODOLOGY

3.1 General philosophy of the alignment

In order to be properly aligned, a light ray that enters the K-mirror superimposed to its mechanical rotation axis, shall emerge also superimposed to the mechanical rotation axis at the output as well. That condition is both necessary and sufficient to fulfill the internal alignment of a K-mirror.

The mechanical rotation axis is thus the backbone that will drive the alignment. Obviously, the mechanical rotation axis is invisible and any attempt to determine its position mechanically may end up with a final alignment precision which is bounded by the precision of its mechanical determination. Our alignment method proposes to determine its position by an optical way, together with the alignment procedure, with as a result a sub-diffraction accuracy.

We will not attempt to send any ray of light along the mechanical axis, because any laser beam –as small as it may be– is too gross for our purpose. An axis is defined by two points (preferably as distant as possible one from the other for a better definition of the axis). Our two point-sources will be of a sub-diffraction, micrometric size: one is located close to the K-mirror entrance (few centimeters) –and we call it the “*field*”, the other at infinity (or close to) that we call the “*pupil*”. The names (field and pupil) refer, by similarity, to the beam the K-mirror will work on at the ELT. Using a system of fixed beam-splitters, those two points will be observed through fixed optics and through the fixed K-mirror body by fixed cameras: one camera for the field, another one for the pupil. Everything is fixed, except the prism and the flat mirror that are to be aligned, and the two sources that will be brought by the alignment procedure right onto the mechanical rotation axis. The procedure is simple because the optical setup is simple, and all the main elements (K-mirror, optics, cameras) are all static.

When misaligned, a rotation of the K-mirror on its axis induces on both cameras a motion of each source following an arbitrary epicycloid trajectory, different for pupil and field. The goal of the alignment is that each camera observes a fixed Airy pattern rotating on itself during a full revolution of the K-mirror, the way to achieve it is explained in 3.3.

3.2 Test bench

In order to align the K-mirror and test its performance, a test bench has been set up that simulates an even faster beam ($f/20$) than the ELT’s optical beam (that will be $f/30$) (Figure 6). A $f/20$ beam allows us to get smaller diffraction pattern, hence an increased precision. Since the K-mirror rotates the whole beam, i.e. field and pupil, the setup needs two optical

paths: a source at ‘infinity’ (or, at least, at a large distance) for pupil simulation and a source just at the K-mirror entrance and re-imaged in a $2f=2f$ setup for field simulation. All sources are LED-fed fibers at $\lambda \approx 630$ nm.

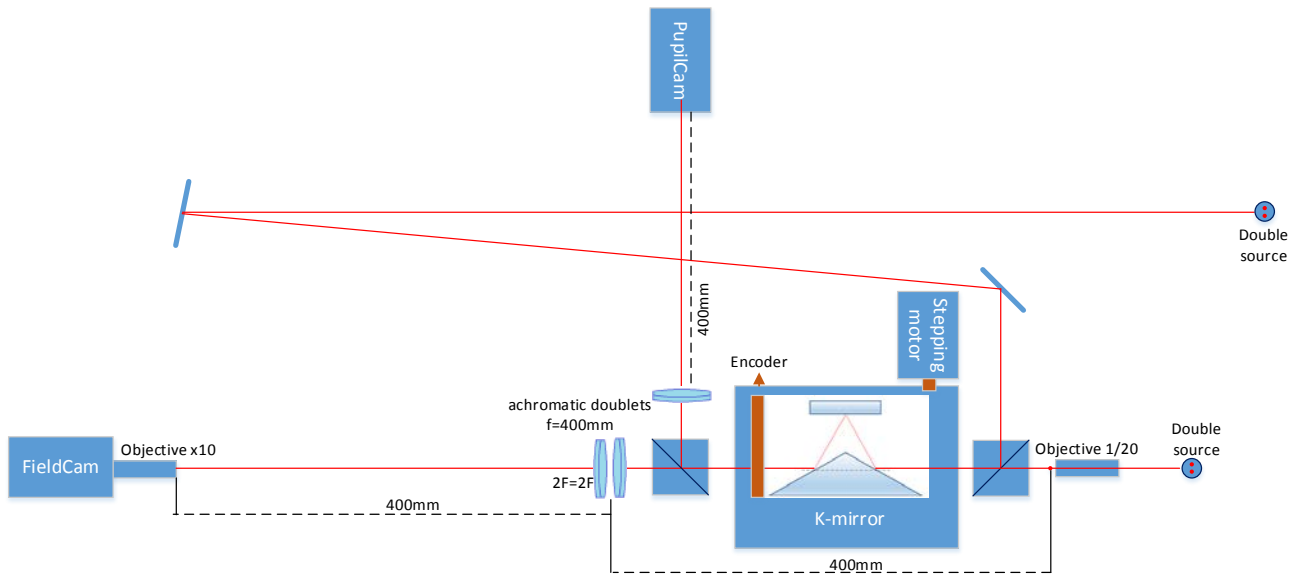


Figure 5. Optical test bench of the K-mirror prototype. Two cameras are observing through the K-mirror. Each camera is observing its own double-source, one very close to the K-mirror entrance, the other placed far away.

Aligning the K-mirror means merging the optical axis on the mechanical rotation axis. In order to do this, the point-source of each optical path (field and pupil) is actually a narrow double source on a movable X-Y mount so that the centre of the rotation can be distinguished. Each source is like a double star, and the separation shall be of the order of some few λ/d , or few dozen λ/d . The small separation of the double source is made possible with custom made MTP optical fiber head connectors of USConec (Figure 6) that was available in the lab. The fiber heads of the double source at ‘infinity’ have a diameter of $195\mu\text{m}$ each and a separation of 2.275mm . The double source for the field simulation has a diameter of $10\mu\text{m}$ each with a separation of 0.1mm . The latter is made possible by re-imaging the fiber bundle using –in reverse– a $\times 20$ microscope objective.

One of the stars in the couple is brighter than the other, and is (arbitrarily) decided to be the central one (the one that shall be precisely set on the mechanical axis). The reason for the other one will be explained in 3.3.

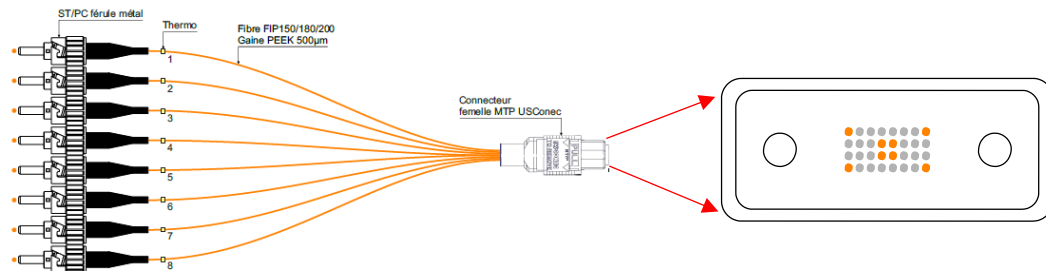


Figure 6. MTP optical fiber head connector to create double sources with a small separation. Fiber heads 1 and 2 are used for the pupil and field optical paths. Their separation is 2.275mm with each a diameter of $195\mu\text{m}$.

Each optical path ends with a CMOS camera with pixel size of $5.86\mu\text{m}$. The diameter of the beam that passes through the K-mirror is 20mm . Achromatic doublets with a focal of 400mm are used, which gives a ratio of about $f/20$ on the cameras. Working at 630nm , the Airy disk is about $\sim 13\mu\text{m}$ wide and will thus be sampled on 2 pixels.

When approaching the very final alignment tuning, where an increased precision is required, a $\times 10$ microscope objective can be added in front of the camera to zoom and oversample the Airy disks.

3.3 Rapid alignment

The image motion made by a misaligned K-mirror turning with a speed θ can be described as a rotation by an angle 2θ around a center, itself permanently moving along a circle at a speed θ . This creates pretty epicycloids, unfortunately quite undesirable. The rotation of the image between two position angle of the K-mirror is always a rotation, made around a center which location is moving and misalignment-dependent. When the K-mirror angles are chosen to be 0° , 120° and 240° , the 3 rotation centers C1, C2, C3 are always located on an equilateral triangle which center O is the image of the **real** mechanical rotation axis in the output space. The 3 points, symmetric to C1-2-3 by O, are the positions of the image of the real mechanical axis through the K-mirror in the input space.

The point in having a couple of sources instead of a single one is the following: the parameters (angle and center) of the transformation of an image by a rotation of unknown center can be entirely determined as soon as the positions of at least two points of the image can be measured. We have developed a software able to recognize automatically where spots are, identify which spot is which thanks to their relative intensity, identify their precise position on the camera using a correlation-based algorithm with a peak detection and interpolation leading to sub-pixel accuracy (errors smaller than 0.01 pixel rms are routinely achieved). Using pairs of coordinate couples, the software can determine in an automated way the center of the rotation.

The two planes, pupil and field, are visualized simultaneously so that both the prism and the flat mirror are aligned at the same time. The idea is to put the brightest source of the couple right on the rotation axis that becomes visible by rotating the K-mirror. A first rapid alignment is done by registering the positions of each source (S1 and S2) at 0° , 120° and 240° . For each rotation the rotation center is calculated, which gives three points C1, C2 and C3 which are located on a circle at 120° from each other. With these values the final rotation center on the camera is determined. This center "O" is the position where we expect the exit axis once the K-mirror is aligned. The software puts a red overlay marker (cross) at that location, on top of a "real-time" image display, both for pupil and field.

The positions of the points C'1, C'2 and C'3 are also determined; they are the misaligned images of the entry axis by the K-mirror. They are on the same circle as above but opposite to C1, C2 and C3 with respect to O. The software puts a blue overlay marker (cross) at the location of C'3, corresponding to where the rotation axis is in the source space, on top of the real-time image display, both for pupil and field.

First step of the alignment is to bring the brightest source of the pupil and of the field superimposed at the calculated "blue" entry axis marker by moving the X-Y mount of the source itself. The operation is done manually by the operator by looking at the real-time display. That is really easy, and ensures that pupil+field sources are now located right on the mechanical rotation axis. Then the next step is to bring the sources (pupil and field simultaneously) at the exit axis "O" using the four degrees of freedom:

- alignment of the pupil image by changing height and rotation of the prism
- alignment of the field image by changing θ and ϕ of the flat mirror

When the bench is ready, the full procedure to align the K-mirror takes only few minutes. It is easy because the alignment of the sources is separated from the alignment of the K-mirror itself, and the degrees of freedom to align the mirrors are nearly de-coupled between pupil and field.

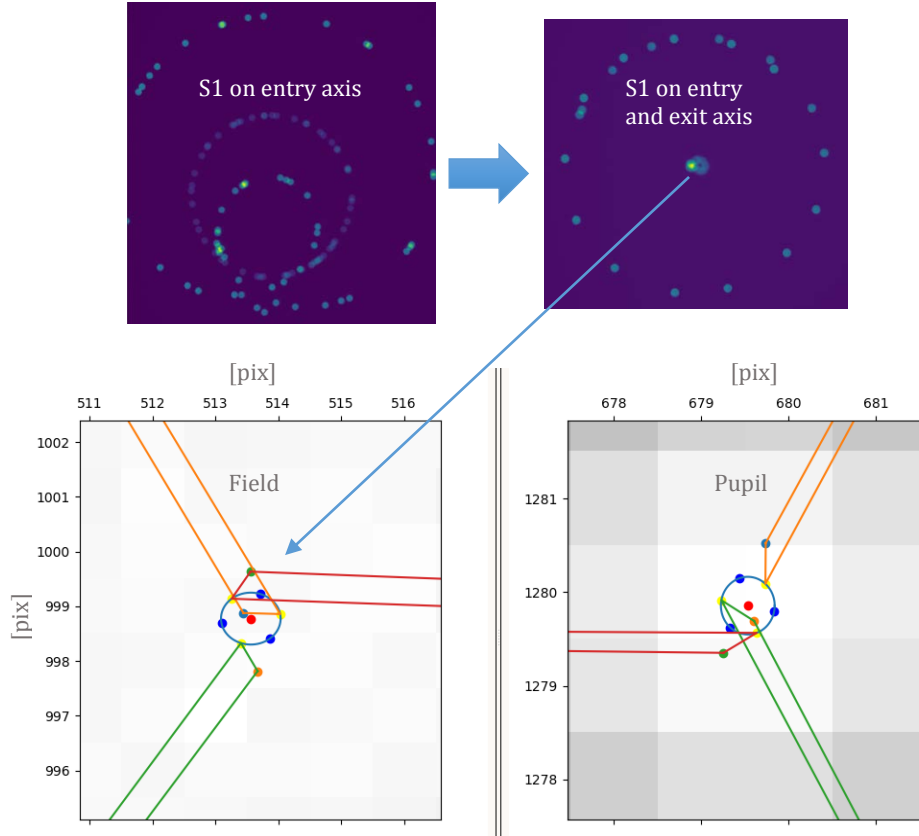


Figure 7. After alignment the reference source (S2) should rotate in a circle around the rotation axis and the central source (S1) located on the rotation axis has an alignment error of less than a pixel.

3.4 Precise alignment

The previous alignment is said “rapid” because it only takes few minutes, and only requires 3 positions at 120° of the K-mirror angle. The precision obtained after applying the procedure a few times could be sufficient for most of the K-mirrors. However, we aim at doing better.

As shown in Figure 7 : when the bright central fiber S1 is aligned on the entry axis of the K-mirror the shape that is created is a perfect circle around the exit axis and the figure of the image of second point S2 is a cardioid (a specific type of epicycloid). The behavior of the source rotating around a central point can be described with a 2-term Fourier series.

$$X_0 + R_1 \cos(\alpha + \varphi_1) + R_2 \cos(2\alpha + \varphi_2) \quad (1)$$

$$Y_0 + R_1 \sin(\alpha + \varphi_1) + R_2 \sin(2\alpha + \varphi_2) \quad (2)$$

where:

X_0, Y_0 the coordinates of the rotation center (or offset)

R_1 the radius of the first circle (from center to S1)

R_2 the radius of the second circle (from S1 to S2)

α the rotation angle and φ_1 and φ_2 the phase of S1 and S2

So to align the K-mirror we can also fit the shapes of the images of S1 and S2 by a cardioid function (2-term Fourier series) and find their respective rotation center. So for the rotation center of the entry axis we have:

$$X_e = X_0 + R_1 \cos(\alpha + \varphi_1) \quad (3)$$

$$Y_e = Y_0 + R_1 \sin(\alpha + \varphi_1) \quad (4)$$

By fitting the positions of the images of S1 and S2 after one rotation, the error between the fit and measurement (4th order term) can be visualized (Figure 8). This error is the difference between the measured trajectory and the best “cardioidic” fit, and it is very small. Its particular shape cannot –in principle– be generated by a misalignment of the 3 mirrors. It is induced by other second-order effects, such as

- the internal mechanical flexures of the mirrors moving under their own weight while the rotor is turning,
- or such as modifications of the position or direction of the mechanical rotation axis with the rotation angle due to some wobble of the bearings,
- or anything else we have forgotten and that makes the mechanical rotation not to behave as ideally expected.

Using this method, we now can identify which part of the measurement is not caused by a pure misalignment, and work on the mechanical design to improve it. It turns out that our first tests have regularly shown an error figure with the shape of a “4-leaf clover” that we have tried to reduce to zero using the mechanical design presented in 2.2.

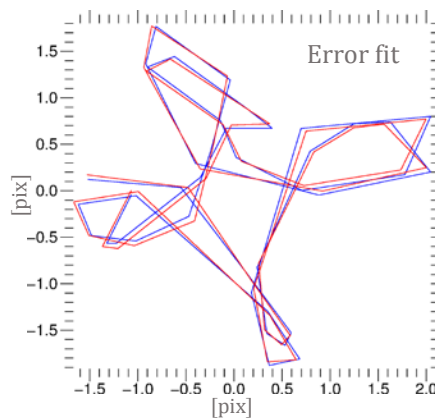


Figure 8. Example of a residue between and best epicycloidal fit and measurement (‘four leaves clover’)

Ultimately, when the “4-leaf clover” shape is reduced to zero thanks to a well-adjusted mechanics, we are just left with the nanometric mechanical imperfections of the bearings. The motion of the fiber images is no more a smooth or regular trajectory but looks more like a random motion.

4. PERFORMANCE

The latest motorized version has proven a great ease of alignment. It has a good stability during alignment and in time and mechanical limitations such as flexures and bearing wobble have been overcome.

4.1 Alignment precision

After alignment we obtain sub-pixel precision between the optical and mechanical axis. The shape of the image after one rotation can no longer be fitted with an epicycloid; it is more like a wobbling circle.

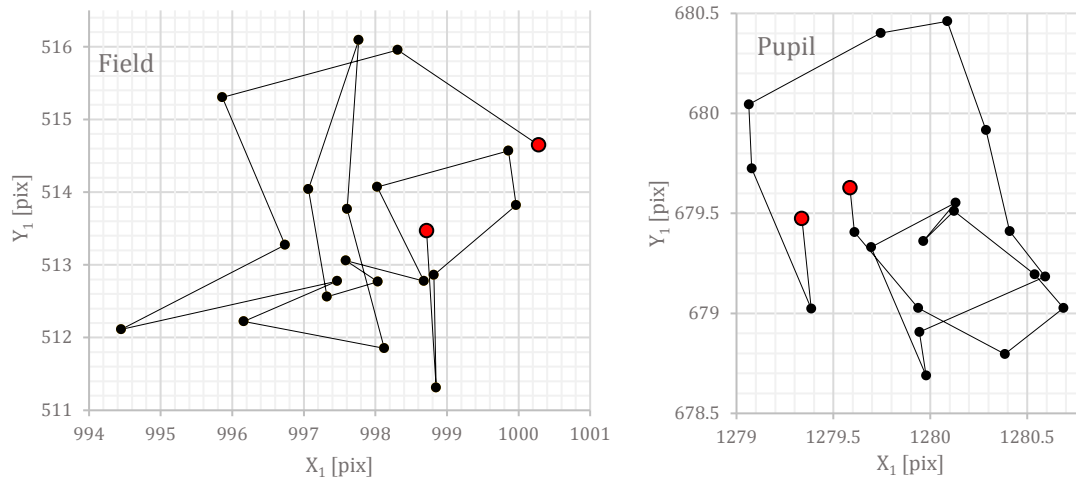


Figure 9. Positions of the field (left) and pupil (right) after one rotation. The field image is magnified by 10! One pixel is $5.86\mu\text{m}$.

The ‘diameter’ of this shape for the field image is less than $3.5\mu\text{m}$ peak-to-peak ($= 6\text{pix} \times 5.86\mu\text{m}/10$; where 10 is the magnification in front of the field camera) or 0.62 mas on sky. The Airy core of the ELT (FWHM at $1.65\mu\text{m}$ and $f/30$) has a diameter of $50\mu\text{m}$. The figure below visualizes that the wobble of the field is well below the core diameter.

The diameter of the wobble of the pupil image is less than $30\mu\text{rad}$ peak-to-peak which corresponds to 0.1% of the ELT pupil diameter. Representing the E-ELT pupil at the same scale as the pupil error of figure 9 would require to draw the E-ELT pupil of the figure below with a diameter of about 70 m (assuming that document printed on A4 format).

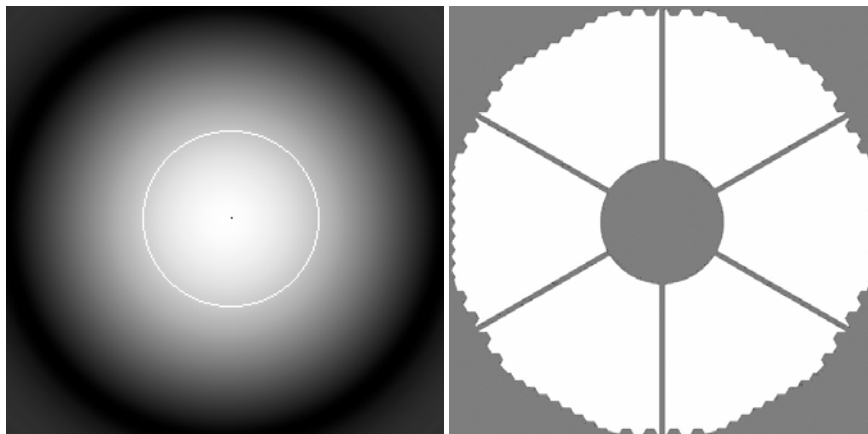


Figure 10. **Left:** Simulation of the wobble (tiny black dot in the middle) within the Airy core of the E-ELT in H-band with $f/30$. **Right:** Pupil simulation of the E-ELT.

The shape of the measurement in figure 9 can no longer be fitted by an epicycloid. The positioning of the three mirrors is so small that it is dominated by all other mechanical errors such as the friction and bearing imperfections, flexures during rotation due to gravity changes, etc. The performance of the K-mirror is so high that it is much better than the initial specifications.

4.2 Angle precision

We also compared the angle position given by the Heidenhain angle encoder and the angle calculated from the positions of the double source (S1 and S2). In order to have a higher precision, we used the source at infinity (for a bigger lever arm), we increased the separation between the fibers of the double source and shifted the CCD to have both images of S1 and S2 on its surface. A separation between the fiber sources of the pupil of about 100mm was needed to get about 1800 pixels between S1 and S2 on the CCD. With this lever arm, one pixel corresponds to 0.016° in the angle measurement. A

rotation of 15° was possible within the surface of the CCD (1936×1216 pix). This measurement was repeated four times from 80° to 95° .

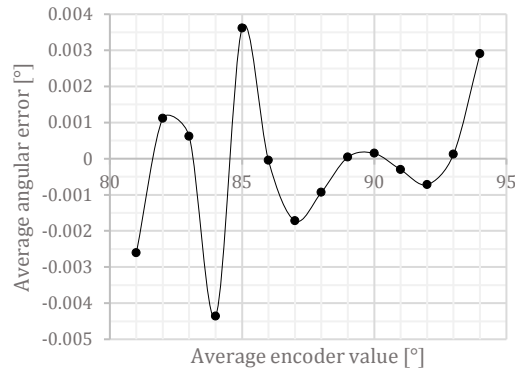


Figure 11. Average angular variation of fiber S2 of the pupil image regarding the average encoder angle

The central image S1 moved slightly between the measurements of 1 to 2 pixels, but the radius (distance rotation centre - S2) stayed within an error of one pixel. The angular variation of the fiber image S2 regarding the encoder is between -0.005° à $+0.004^\circ$ (see Figure 11).

4.3 Stability and hysteresis

For the stability tests we are merely interested in the pupil image, which is most impacted by variations; the optical path length from source to camera causes a bigger lever arm for instabilities and the prism is more sensitive to mechanical flexure than is the flat mirror.

The test bench is affected by day and night temperature fluctuations. The measurements are difficult when it comes to disentangle the drifts coming from the K-mirror alone from those coming from the bench. Several measurements over ≈ 30 to 50 hours have been done, sometimes showing non-consistent results (bench drifts larger than K-mirror) because the measurement runs were performed under different meteorological conditions. As the drifts induced by the K-mirror are very small (probably smaller than those induced by our bench), a great attention has to be paid to temperature measurements too. We are currently in the process of measuring those drifts together with the temperature of several elements in the setup in order to identify in the detail which are the real contributors. However, first numbers are extremely encouraging and give an order of magnitude. Figure 12 shows the drift of the position of the source (X_1 , Y_1) of the pupil on the camera during a 50h measurement during the week-end. The measurement is done with the K-mirror installed in the test setup. The drift speed is –at worst– of 1 pixel ($<6\mu\text{m}$ for field and $<15\mu\text{rad}$ for pupil) per day. Thanks to other measurements done with several PT100 probes on the test bench, we can conclude that the day and night fluctuation is due to a perfectly similar temperature fluctuation.

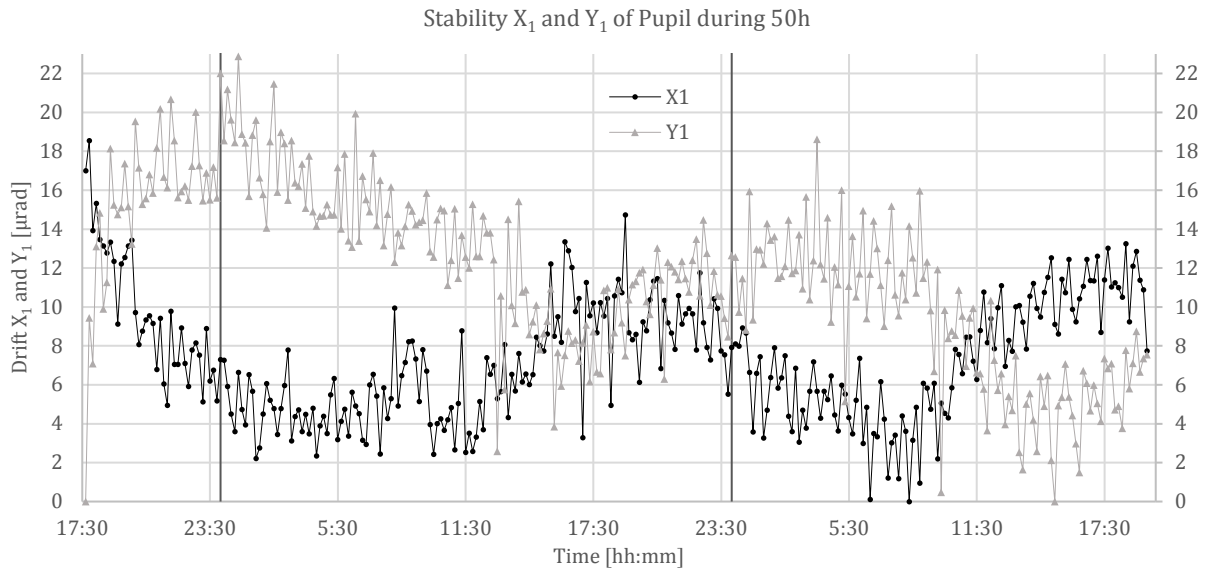


Figure 12. Example of drift measurement of fiber positions X_1 (black) and Y_1 (grey) of the pupil (one recording each 15min during 50 hours). The black vertical lines are at 0h.

A second stability measurement is obtained by plotting each hour the position (X_0, Y_0) of the rotation center of the K-mirror. Instead of registering the fiber positions, the K-mirror performs a full rotation once an hour and its rotation center is calculated using the cardioid fitting function (see paragraph 3.4) and plotted against time. For this measurement we could not distinct a correlation between temperature and drift, but we plan to perform the same measurement with more, and more precise pt100 probes on the test bench.

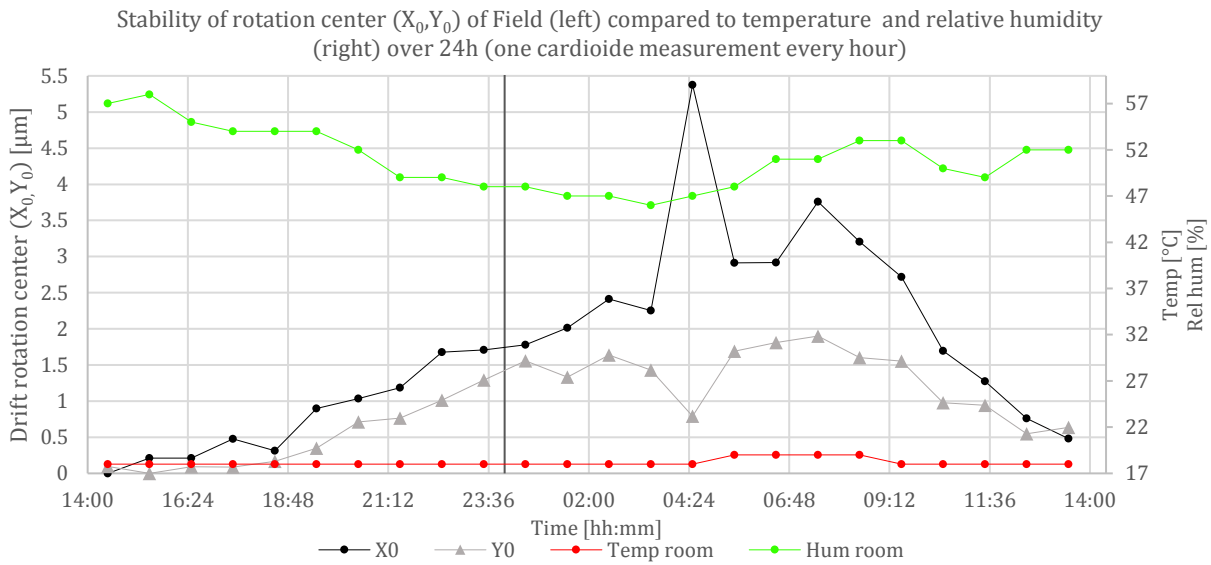


Figure 13. Rotation center positions (black, grey) compared to temperature (red) and relative humidity (green) in the cleanroom

A final stability test is performed to verify the hysteresis of the K-mirror rotation in both directions. We chose to show the position (X_2, Y_2) of the second fiber S2, since its shape after one rotation is a quasi-perfect circle. A shift between clockwise and counterclockwise is much easier to detect.

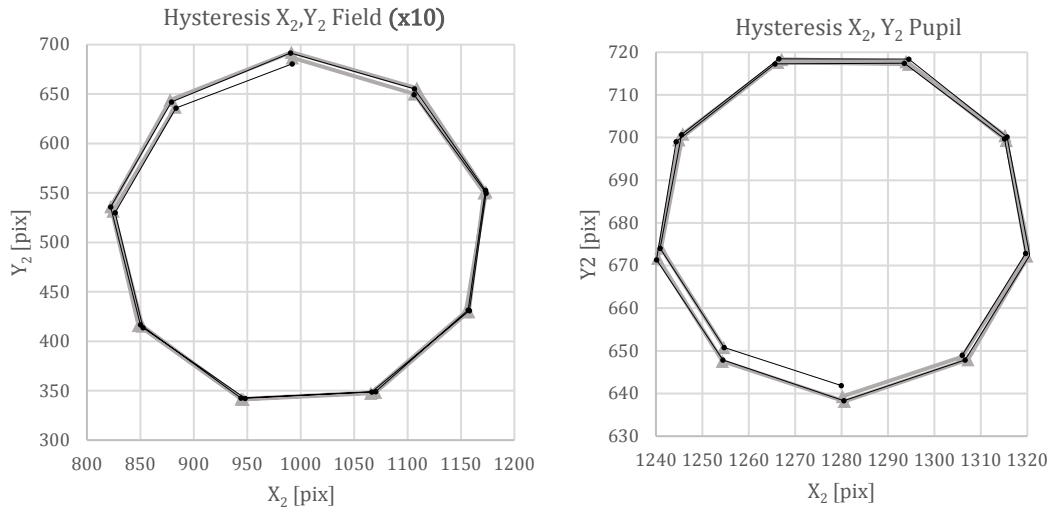


Figure 14. Fiber positions (X_2 , Y_2) of the second fiber S2 during a counterclockwise (black) and clockwise (grey) rotation of the K-mirror: Field (left) and Pupil (right).

The error between counter and clockwise rotations is less than $1.2 \mu\text{m}$ in X and Y for the field, and $44 \mu\text{rad}$ in X and Y for the pupil.

4.4 Optical path shift induced by K-mirror

The optical path shift induced by the K-mirror has been measured. The theoretic shift with $H=30\text{mm}$ is 34.64mm . On the test bench we measured a shift of 34.36mm , which means that when removing the K-mirror we have to elongate the camera from the optical source with 34.36mm to have a focused image. The deduced height H is 29.75mm , which is coherent with the mechanical tolerances of the structure.

5. PERSPECTIVE

It has been demonstrated that the alignment of the mirrors can be brought to sub-micron accuracy and fulfills the specifications. Elements that still need to be studied now are the long-term stability and the influence of the temperature. Therefore, thermal tests from -15°C to 25°C will be achieved in a thermal chamber in order to detect the parts that are most temperature sensitive and to measure the impact on the mechanical alignment and optical quality.

After the final design review (end of 2020) of the MICADO SCAO project, a final version of the K-mirror will be manufactured. Mid-2022 the K-mirror will be installed in the AIT setup of the SCAO WFS, which means that at least 2 years are still available to fine-tune the design and converge to a non-thermal one.

REFERENCES

- [1] Davies R., Alves J., Clénet Y., et al, “The MICADO first light imager for the ELT: overview, operation, simulation”, Proc. SPIE, 10702, (2018)
- [2] Clénet Y., Buey T., Gendron E., et al, “The MICADO first-light imager for the ELT: towards the preliminary design review of the MICADO-MAORY SCAO”, Proc. SPIE, 10703, (2018)